3-3-2 A Millimeter-Wave Broadband Wireless Access System Using Mobile Tracking Technology

Hiroyuki TSUJI and Hiroyo OGAWA

We describe a new system for high-speed wireless access systems between base stations and mobile terminals. In the proposed system, the base stations are located along street or in public facilities and formulate the antenna beam toward mobile terminals to utilize the millimeter wave efficiently. The base station has an array antenna and tracks mobile terminals by using a new tracking algorithm. A radio-on-fiber technique is used to simplify and miniaturize the components of the base station. We propose a new tracking algorithm that uses directions-of-arrival, angular velocities of mobile terminals, and scatter modeling in multipath communications channels to improve the tracking performance. We also developed experimental equipment to demonstrate the feasibility of the proposed millimeter-wave broadband wireless access system and the efficiency of the tracking algorithm using an array antenna system. Finally, we discuss our simulation and experimental results.

Keywords
millimeter-wave, array antenna, radio-on-fiber, direction-of-arrival (DOA)

1 Introduction

There has been growing interest in recent years in expanding broadband network services to the users of wireless terminals through a wireless communications system[1]~[4]. Such a wireless access system will require high-throughput data-transmission technology for a seamless interface between the wired and wireless networks. Low-frequency bands with frequencies lower than that of the microwaves are already occupied by conventional applications, and in many cases involve limitations on the available bandwidths. Under these circumstances, a wireless communications system using the millimeter-wave band has been attracting attention, since millimeter waves have considerable available bandwidth space for easy high-speed communications. In addition, short wavelengths enable use of compact antennae and other hardware components[5]. On the other hand, millimeter waves are easily blocked by buildings and other structures and are subject to attenuation by air[3]. In addition, compared to other wireless communications systems, millimeter-wave systems offer coverage of only small service areas (cells). This necessitates a large number of base stations, increasing construction costs. In order to maximize the advantages of millimeter waves to solve the above problems, we propose an innovative communications system utilizing radio-on-fiber and array-antenna technologies[6]. Each base station of this system, is equipped with an array antenna or direction-selectable antenna to provide the maximum gain in the direction of a desired signal and to mitigate interference with the other terminal stations. The radio-on-fiber technology is used to simplify and downsize the constituting components of the base station. This technology allows the control station to control the array antenna of the base station directly by connecting the control station with the base station through an optical fiber and using the wavelength-division-multiplexing subcarrier. The radio-on-fiber and array-antenna technologies provide the mil-

limeter-wave based wireless access system with a number of advantages. However, the implementation of this system poses several challenges. For example, in systems in which the mobile terminal may approach the base station and be used in the operation of vehicles, the direction-of-arrival of signals sent from a mobile terminal change significantly over time. This makes it difficult to direct the antenna beam toward the moving terminal. In addition, when the mobile terminal is moving quickly, the error in estimating the direction-of-arrival of signals sent from the mobile terminal will become large if that estimate relies on conventional algorithms. This is because the covariant matrix of the data received by the array antenna must be calculated to estimate the direction-of-arrival. In order to solve these problems, a new mobile-terminal tracking method has been developed. This method utilizes information on the direction-of-arrival and angular velocity of the mobile terminal [7]. If these two parameters are used, the tracking performance can be improved even when the mobile terminal moves very quickly, compared to conventional direction-of-arrival estimation methods. We have developed an algorithm that enables real-time processing and takes into account scattering around the mobile terminal by improving the proposed algorithm[8]~[11]. This is because that the original algorithm, which uses a model that does not account for multipathing, is not capable of precisely estimating the direction-of-arrival when the mobile terminal is used in an environment of multipath communications channel.

This paper describes a new broadband wireless access system incorporating the improvements referred to above. Among the important component technologies proposed for the implementation of the new system, we focused on its capacity to track a mobile terminal utilizing the array antenna and wavelength-division-multiplexing technology. This tracking system places a priority on a direction-of-arrival estimation algorithm that can improve tracking performance, even in a multipath environment. To demonstrate the effectiveness of the proposed mobile-station tracking system, we conducted simulation studies and developed devices, including the array-antenna and wavelength-division-multiplexing transmission system, for field experiments.

This paper consists of the following sections: Section 2, which explains our system concept; Sections 3 and 4, which describe the primary technologies for the antenna design of the mobile-station tracking system and the wireless access system for millimeter waves; Sections 5 and 6, which describe the algorithm for mobile-station tracking and demonstrate its effectiveness through simulations and field experiments; and a summary of the conclusions.

2 Outline of the broadband wireless access system

This section describes the details of the proposed broadband wireless access system. Fig.1 illustrates the concept of the proposed system. In this system, each base station has an array antenna or direction-selectable antenna. The array antenna directs its antenna beam in the desired signal direction after estimating the direction-of-arrival of signals sent from the mobile station for high-speed communication. However, it also directs the nulls of the antenna beam in directions that may cause interference. This is the procedure for increasing the power of the desired wave while removing interference waves from the received wave. Base stations are installed at intervals of 50-100 m along streets in order to maintain line-of-sight communication between the respective base stations and terminal stations. This system employs macro diversity (or site diversity) technology. When the direct path to a base station is interrupted by an obstacle, the mobile terminal begins communications with another base station with which a direct path can be secured.

The implementation of the above system poses several challenges. First, compared to other wireless communications systems, the

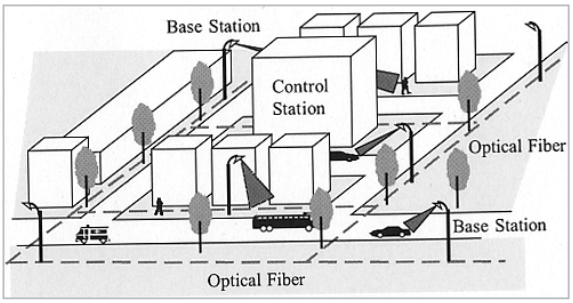

Fig.1 *Schematic drawing of the system concept*

construction of base stations involves significant time and expense. This is partly due to limitations on the available space for the installation of base stations. As a potential solution to this problem, radio-on-fiber technology has been attracting attention for its ability to transfer the signal information received at the base station to the control station as is[12]. If this technology is employed in the wireless communications system, the base station does not require the installation of complex hardware such as a line control switch or modem, which can be integrated into the control station.

Second, as shown in Fig.2a, we propose a new configuration of the base and control stations for controlling the array antenna. In the reverse link, the output signal from the array antenna directly modulates the intensity of optical signals, and the signals are sent to the control station through an optical fiber. The structure of the reverse link is virtually the same as that of the forward link. In the forward link, the signals divided in the modulator directly adjust the intensity of optical signals, and the signals are sent to the base station through another optical fiber. However, if the same structure is used for both the reverse and forward links, several problems may arise in the forward link. For example, it is difficult to form a beam with a narrow beamwidth at a high gain. If the array antenna is used to realize such a beam pattern, the total number of antenna elements must be increased. However, if the number of elements is increased, the stages of multiplexing in the wavelength-division multiplexer increase, making the system itself more complex. In addition, the calibration of the array antenna used in the forward link is generally difficult to perform compared with the calibration during signal reception. We therefore propose another configuration of the base and control stations, as shown in Fig.2b. The array antenna is used only to estimate the direction-of-arrival of signals sent from the mobile terminal. A direction-selectable or sector antenna is used in communications, allowing the antenna direction to be changed in accordance with information on the direction-of-arrival. While the configuration shown in Fig.2b is easy to implement and provides high antenna gain, the degree of improvement in communications quality due to the elaborate beam control will be limited, since complex beamforming is difficult to implement.

In the proposed antenna configuration, virtually all of the hardware components, including those for beamforming, handover, and modulation/demodulation, can be integrated into the control station. Since a high-performance digital signal processor (DSP) can be installed in the control station, the base station can in turn be made even move compact. If a better DSP has been developed, the DSP unit of the control station can easily be replaced. A more sophisticated algorithm is available for the control of the array antenna without retrieving the base station.

3 Antenna design for the millimeter-wave access system

3.1 Investigation of antenna structure

This section describes the antenna design for estimation of the direction-of-arrival and the configuration for the implementation of communications between the base station and the mobile terminal. First, the required specifications for the antenna are investigated. Our system greatly depends on the behavior of the direct and reflected waves during the signal exchange between the base station and the mobile terminal. However, this study considers only a single direct wave to simplify

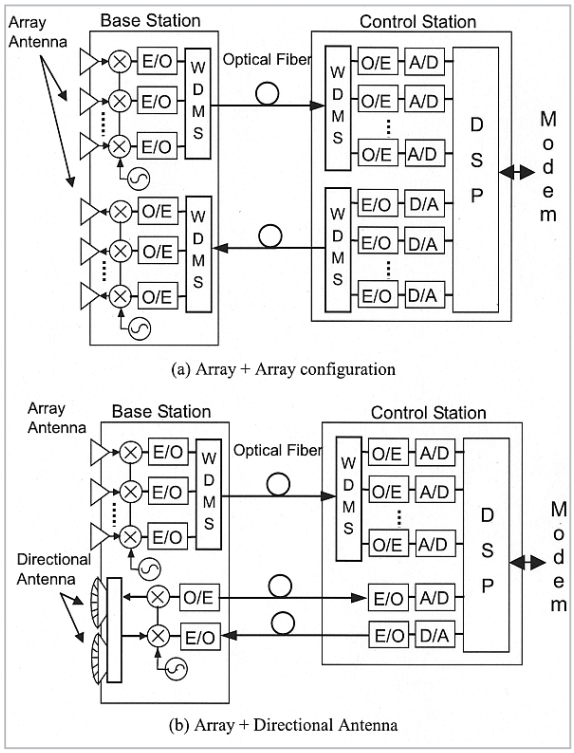

Fig.2 *Configuration of the base and control stations for array signal processing*

design of the antenna structure. We designed the antenna under the following assumptions:

- The free-space propagation model will be used.
- The propagation loss caused by the air will be taken into account.
- The central frequency is set to 59.5 GHz.
- The transmission power is set at 10 dBm at the mobile terminal.
- The distance between the base station and the mobile terminal is a maximum of 50 m.
- The antenna of the base station is 5 m in height.
- The CNR (carrier-to-noise ratio) must be at least 5 dB for estimation of the direction-of-arrival and at least 15 dB for communications.
- The NF (Noise Figure) is 10 dB.
- A patch antenna is employed in the mobile terminal and is also used in the base station for estimation of the direction-of-arrival.

For the link budget between the base station and the mobile terminal, we assume a virtual antenna that has antenna directivity (electric-field-strength) that is both vertically and horizontally symmetrical and can be approximated using the *n*-th power of the cosine function[18]. Specifically, the antenna directivity is defined as follows:

$$D(\phi) = (\cos\phi)^{2n} \tag{1}$$

where ϕ is the angle measured from the boresight of the antenna. The following equation is obtained if the half-power beamwidth of the patch antenna is expressed using ϑ:

$$\left(\cos\frac{\vartheta}{2}\right)^{2n} = \frac{1}{2} \tag{2}$$

For example, if ϑ = 80 degrees, n = 1.3. In addition, if the front gain of the antenna is defined as a function of the half-power beamwidth of the antenna[19] as shown below:

$$G_f = 10\log_{10}\left(\frac{K_g}{\vartheta_H \vartheta_V}\right) \tag{3}$$

where K_g is a constant with no unit and ϑ_H and ϑ_V are the half-power beamwidths (degree) along two perpendicular axes (the horizontal and vertical axes). If K_g is set to 24000, the front gain G_f is calculated as 5.74 dBi assuming ϑ = 80 degrees. Equations (2) and (3) result in the following mathematical model for antenna gain:

$$G = G_f + 20n\log_{10}(\cos\phi) \tag{4}$$

where ϕ is the direction-of-arrival of a wave arriving from the base station or mobile terminal. Equation (4) can thereby simulate a patch antenna with a wide beamwidth and a horn antenna with a narrow beamwidth by changing the magnitude of ϑ.

CNR is finally defined by equation (5) as follows:

$$\mathrm{CNR} = P_T + G_T + L_{free} + L_{oxgn} + G_R - N_P \tag{5}$$

where P_T is transmission power, G_T the antenna gain on the transmission side, and G_R the antenna gain on the reception side. N_P, the noise power, is –87 dBm when the bandwidth is 1 MHz and NF = 10 dB, while it is –104 dBm when the bandwidth is 50 MHz and NF = 10 dB. L_{free} and L_{oxyn} are free-space propagation loss and oxygen absorption loss, respectively, which are obtained by $20 \log_{10}(\lambda/4\pi r)$dB and –16 dB/km. G_T and G_R can be calculated by equation (4). The CNR for the base station is calculated from these parameters.

3.2 Cell arrangement

This section describes the cell arrangement for communications between the base station and the mobile terminal and for estimating the direction-of-arrival. Fig.3 demonstrates the two types of cell arrangements we propose. One is a single-side-radiation system that covers either the left- or right-side area of the base station. The other is a both-side-radiation system that covers both sides of the base station. These systems have the following features:

Single-side-radiation system

– The propagation distance is large.
– Signal power is efficiently utilized.
– Multi path effects may be enhanced.

Both-side-radiation system

– The propagation distance is small.
– The probability of signal blocking is low.
– The electric fields at both cover edges are weak.
– The antenna beam must be switched at the mobile terminal when the terminal passes under the base station.

The arrangement of base stations should also be considered. In general, the base station is located directly above the street or at roadside.

It is of great importance in the present study to determine the angles of the boresight of the base station and mobile terminal, as shown in Fig.4. We have calculated CNR, assuming several possible angles.

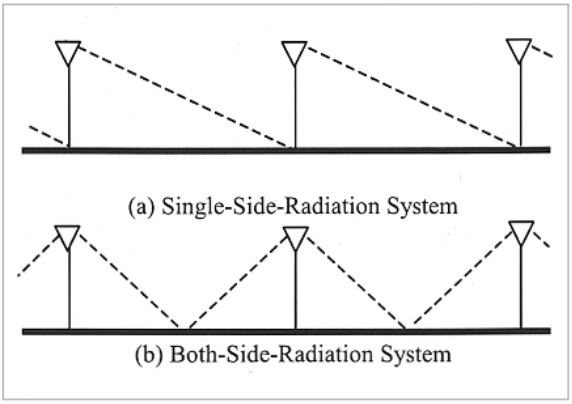

Fig.3 *Cell arrangement*

3.3 Required CNR level for estimation of the direction-of-arrival

Assume that the patch antenna is used at both the base station and mobile terminal for estimating the direction-of-arrival of signals sent from the mobile terminal. As previously mentioned, CNR must be at least 5 dB to estimate the direction-of-arrival, which is a predetermined value limited by the algorithm to be proposed in Section 5. Since the algorithm for estimating the direction-of-arrival does not include processing such as demodulation or synchronization, almost all signals, including special signals (such as pilot signals), control signals transmitted from the mobile terminal, and communication signals exchanged between the base station and the mobile terminal, can be utilized in the estimation of the direction-of-arrival. Assuming that the bandwidth required only for estimation of the direction-of-arrival is 1 MHz, CNR can be calculated as follows:

(A) Both-side-radiation system

First, assume that the base station is installed directly above a street (y = 0). The antenna angles are fixed at $\phi_B = \theta_B$ = 0 degrees so that both sides of the station can be covered as shown in Fig.4 and ϕ_M = 0 degrees. When the mobile station is x = 25 m from the base station, G_R of the base station located in the direction of the mobile terminal becomes –12.65 dBi. Therefore, CNR on the receiving side at the base station is given by:

$$\mathrm{CNR} = 4.80 + G_T \tag{6}$$

This result implies that G_T on the transmission side must be at least 0.20 dBi to attain the CNR = 5dB required for estimation of the direction-of-arrival. However, since the actual G_T of the mobile terminal in the direction of the base station is –12.65 dBi, the required CNR level cannot be attained. Fig.5(a) shows CNR calculated using equation (5), with the distance changed between the base station and the mobile terminal. Figs.5(b) and 5(c) show CNR for cases in which the angle of the boresight of the mobile-terminal antenna ϕ_M = 60 degrees and 80 degrees. That is, only the antenna of the mobile terminal is directed toward the base station. These studies indicate that the effective distance between the base station and the mobile terminal is 30 m or less.

(B) Single-side-radiation system

In this case, the two antennas face each other. We calculate CNR by changing the angles of both the base station and the mobile terminal, as well as the location of the base station. The results of CNR calculation for a case in which the base station is located above the street are shown in Figs. 6(a)/6(b), while those for a case in which the base station is located at roadside (y_0 = 0) are shown in Figs. 6(c)/6(d)/6(e)/6(f). The figures indicate that sufficiently high CNRs are achieved for all locations when the base station is installed above the street. On the other hand, when the base station is installed at roadside, the antenna of the base station should be directed toward the mobile terminal such that $\phi_B = \theta_B$ = 45 degrees, in order to cover all service areas. The results of this study indicate that the single-side-radiation system can be used when it is necessary to estimate the direction-of-arrival for all service areas.

3.4 Required CNR level for communications

We assume that CNR must be at least 15 dB when the bandwidth is 50 MHz for the establishment of communication between the base station and the mobile terminal. This is based on the following assumptions:

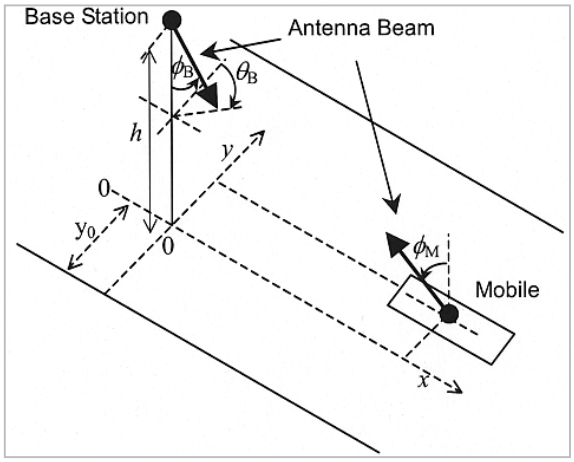

Fig.4 *Definition of antenna angles*

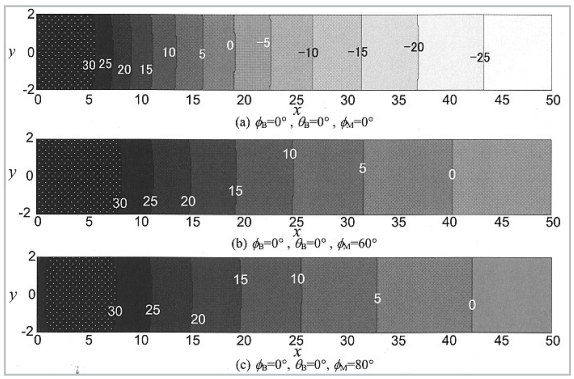

Fig.5 *CNR for estimation of the direction-of-arrival (both-side-radiation system)*

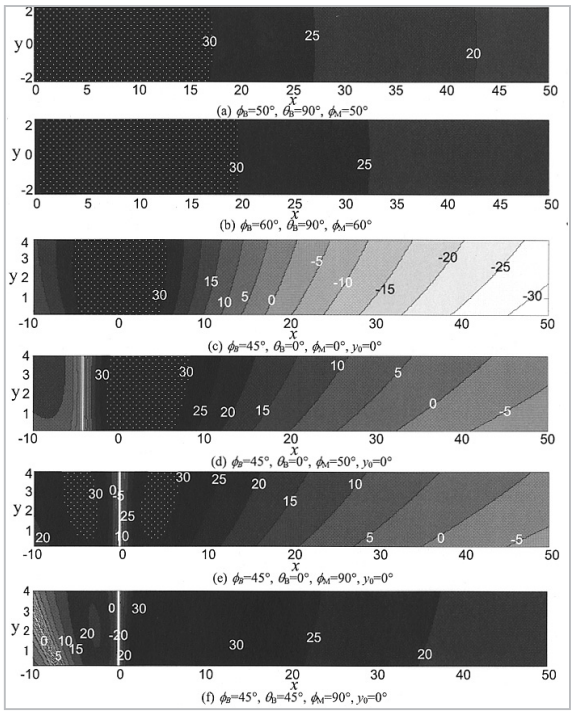

Fig.6 *CNR for estimation of the direction-of-arrival (single-side-radiation system)*

– BER without error-correction scheme is 10^{-5}.

– The modulation mode is single-carrier QPSK.

– Differential detection is adopted.

We have determined the required CNR level in accordance with the CNR versus BER (bit-error rate) table presented in Reference[23].

Next, we will describe the installation angles of the antennas for the base station and the mobile terminal, along with their required specifications.

(A) Both-side-radiation system

Communication between the base station and the mobile terminal requires a bandwidth 50 times that required for estimation of the direction-of-arrival. Thus, the CNR required must be approximately 10 dB greater. If the patch antenna (n = 1.3) is used in the base station of the both-side-radiation mode and the mobile terminal, a complex problem arises. Specifically, if ϕ_B, θ_B, and ϕ_M are set to zero degrees, a sufficiently high CNR cannot be achieved. The antenna of the mobile terminal must be tilted to attain sufficient CNR. This indicates that we must prepare an antenna with directivity that can be switched between its front and rear ends, due to the possibility that the mobile terminal may pass immediately under the base station. However, this system configuration is not suitable for the proposed system, as its control process becomes very difficult to perform. Thus, only the single-side-radiation system is discussed in this paper.

(B) Single-side-radiation system

First, assuming that the patch antenna (n = 1.3) is used at both the base station and mobile terminal, we calculate CNR provided when ϕ_B and ϕ_M are changed.

The results shown in Fig.7 indicate that, when the antenna angle at the mobile terminal is set to ϕ_M = 70 or 80 degrees, a sufficiently high CNR (= 15 dB) is provided in the area within 15 m from the base station if the angle of the base station ϕ_B, is set to either 50 or 60 degrees. Therefore, ϕ_B and ϕ_M must be set to 60 and 80 degrees, respectively, in order to ensure communications between the base station and mobile terminal within 15 m of each other.

Here, we examine a case in which the distance between the base station and the mobile terminal is 15 m or greater. The above study results indicate that the base station is not allowed to use a patch antenna for communications with a mobile terminal located at least 15 m away. Thus, we estimate the antenna gain required to ensure communications when the base station uses another antenna having a different beamwidth or antenna gain.

Assume that the antenna angle at the mobile terminal is set to ϕ_M = 80 degrees based on the results obtained for the estimation of the direction-of-arrival. The antenna angle at the base station is set to ϕ_B = 80 degrees. In other words, CNR is calculated with angles ϕ_B and ϕ_M fixed and the beamwidth at the base station changed. Fig.8 shows the CNR calculation results. Our simulation indicates that communications can be established between the base station and the mobile terminal, which are at least 15 m from each other, if the beamwidth is set to 15 degrees and the antenna gain to 20 dB.

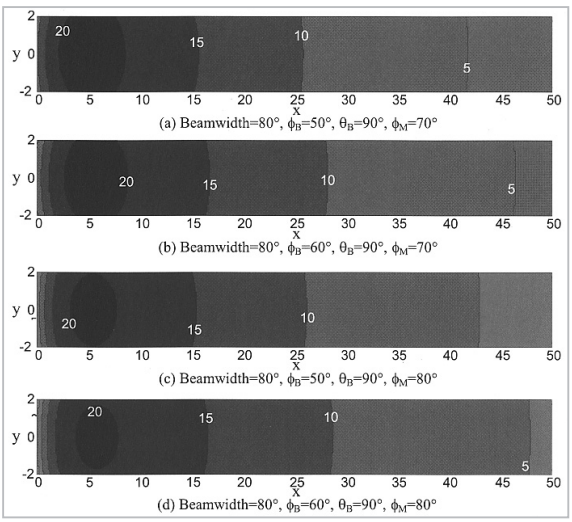

Fig.7 *CNR for communication (single-side-radiation system)*

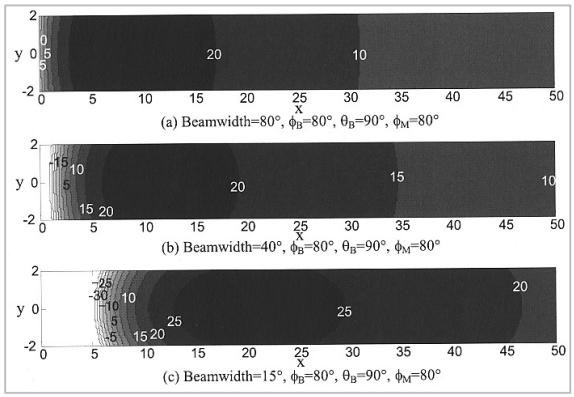

Fig.8 *CNR for an antenna using a narrow beam (single-side-radiation system)*

4 Component techniques for implementation of the millimeter-wave wireless transmission system

4.1 Wavelength-division-multiplexing transmission

Information on the amplitude and phase of signals obtained by elements installed in the array antenna is very important when signals are exchanged between the control station and the base station in the proposed system, because both estimation of the direction-of-arrival and the formation of an antenna beam depend on the amplitude and phase of signals. WDM (wavelength-division-multiplexing) transmission is a suitable technology for signal exchange between the base station and the control station. We have therefore developed a transmission device that adopts the WDM technology used in the proposed array-antenna system[13]. This section provides details on the proposed system.

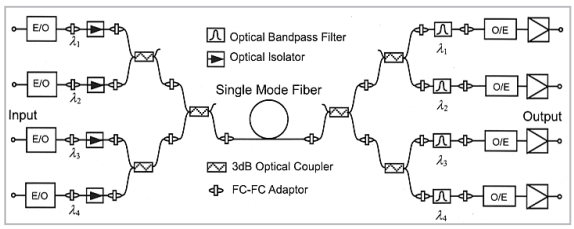

Fig.9 *WDMS transmission system (4 subcarriers)*

Fig.9 illustrates the configuration of the wavelength-division-multiplexing system. This system comprises transducers that convert between optical and electrical signals on different wavelengths, optical couplers that combine multiple optical signals, optical bandpath filters (BPFs), and amplifiers. At the reverse link extending from the base station to the control station, laser diodes of different wavelengths convert between electrical and optical signals that have been received by each element of the array antenna. The outputs are mixed with each other by the optical couplers installed in the base station. After the multiplexed signals are separated into optical signals of different wavelengths by optical couplers and BPFs at the control station, they are restored to their original form by the optical-electrical signal converter. In consideration of the current availability of laser diodes and photo-diodes, we set the intermediate frequency (IF) of this system set to 1.5 GHz. Also, in consideration of the properties of the optical BPF that separates the multiplexed signals, we set the number of multiplexing subcarriers to four. The other specifications are listed in Table 1. If the number of multiplexing subcarriers is doubled, the optical fibers can be shared between the forward and reverse links. However, such a configuration will increase the level of inter-signal interference and the costs for the wavelength-division-multiplexing transmission. We therefore consider it a reasonable option to use two separate fibers for each of the forward and reverse links.

Table 1 *WDMS specifications*

Optical wavelength λ	1298.3mm 1304.2mm 1308.5mm 1315.4mm
Optical Transmission Power	+9dBm
Cross-talk	<−38dB
CNR (m=20%, Bandwidth= 50MHz, Fiber length=4km)	>43dB
Frequency	1.4-1.6GHz

4.2 Millimeter-wave array antenna for the tracking system

At the beginning of this paper, we mentioned that the base station is required to estimate the location of the mobile terminal in order to direct its antenna beam toward the terminal. This section describes the array antenna used in estimating the direction-of-arrival of signals sent from the mobile terminal. A variety of technologies are necessary for the fabrication of an array antenna that utilizes millimeter waves of extremely high frequencies. We have developed an array antenna employing a microstrip antenna (MSA) as the antenna element[14]. The MSA is a suitable component for such an array antenna that has precise element intervals, since it is fabricated by photolithography. As shown in Fig.10, this array antenna has a multi-layer structure. This type of MSA is referred to as an "electromagnetically-coupled microstrip antenna" or a "proximity-coupled microstrip antenna." The central frequency of this antenna is 59.5 GHz. This antenna is a linear-array antenna which has four rectangular patch antenna elements with element intervals of half the wavelength, and. Dummy elements are located on both ends of the element array to make the inter-element coupling uniform. The feed lines in the center layer supply power to the radiation patches through the coupling between the radiation patches and the feed lines.

Using the developed array antenna and the algorithm for estimating the direction-of-arrival, we conducted experiments to estimate the direction-of-arrival in an anechoic chamber. After placing the array antenna on a rotary table, we set the antenna angle at zero degrees. Next, the phase and amplitude of each received signal were adjusted so that the estimated angle became zero degrees (in practice, the complex coefficients of the base-band signal were changed to make the adjustment). In the experiment, the distance between the array antenna and the horn antenna was 3.5 m, and the transmission power was 10 dBm. Upon completion of the parameter adjustment,

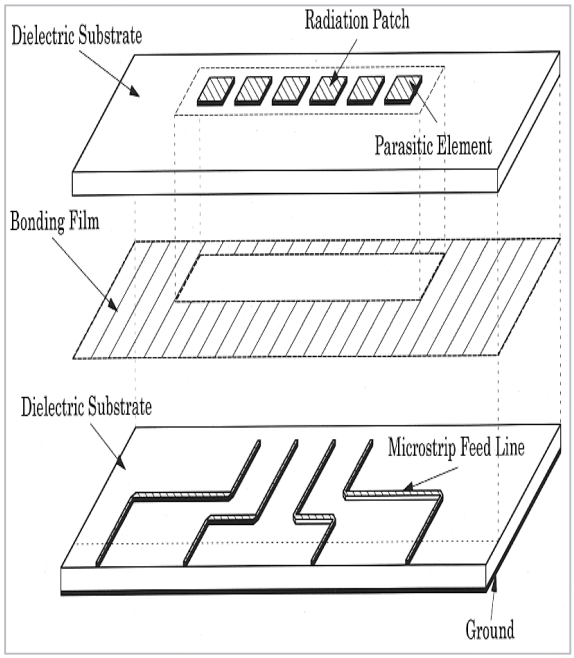

Fig.10 *Structure of the microstrip array antenna*

we measured the direction-of-arrivals at different angles by rotating the rotary table. The measurement results are shown in Fig.11. The results of our experiment indicated that the discrepancy between the actual direction-of-arrival and that estimated was within 3.2 degrees. The standard deviation of estimation errors was 1.6 degrees. We thereby confirmed that the system employing the wavelength-division-multiplexing transmission technology and the array antenna would operate with no problems.

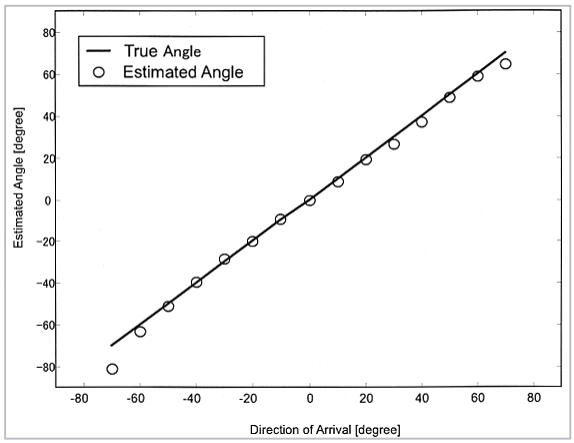

Fig.11 *Estimation of the direction-of-arrival using the microstrip array antenna*

5 Tracking algorithm for the millimeter-wave access system

5.1 Estimation of the direction-of-arrival of signals sent from the mobile terminal

Several methods have been proposed for determining the weight vectors of the array antenna to provide an antenna beam at the base station, in order to optimize communications between the base station and a specific user using an array antenna. The common algorithms used to estimate the direction-of-arrival and to determine the weight vectors are summarized in Reference[16]. One of the recommended beamforming methods is that for determining the weight vectors by utilizing the signal incoming direction (direction-of-arrival). Such a method for estimating the direction-of-arrival can be applied to high-speed communications systems. This is due to the fact that the direction-of-arrival is the only parameter common in the forward and reverse links, making beamforming easy in both links. In addition, although synchronization and demodulation are necessary in such methods that determine weight vectors based on a reference signal, for example, the employed method utilizing information on the direction-of-arrival does not require such processing. It can therefore easily handle high-speed signals. In addition, when a direction-selectable antenna is used in communications between the base station and the mobile terminal, the information on direction-of-arrival can be used to determine the antenna direction. Meanwhile, the estimation of the direction-of-arrival and the determination of weight vectors must be performed separately under this method, which utilizes information on the direction-of-arrival. Thus, we must consider the processing load for these calculations. One of the most important requirements of the proposed system is the precise real-time estimation of the direction-of-arrival for beamforming, even when the mobile terminal moves as fast as a car. This section describes a new methodology for improving the tracking capability of the mobile terminal by introducing the local scattering model presented in Reference[15]. We also demonstrate the effectiveness of the proposed method through a simulation study.

5.2 Signal model

First, a signal model for estimating the direction-of-arrival is explained below. Assuming that N narrow-band plane waves impinge on the array antenna from different directions, $\theta_n(t)$, $n=1,\cdots, N$ where M elements are arrayed in line at equal intervals of D. The received signal can be described as follows in the multipath communications environment:

$$\boldsymbol{y}(t) = \boldsymbol{x}(t) + \boldsymbol{v}(t) \tag{7}$$

$$\boldsymbol{x}(t) = \sum_{n=1}^{N}\sum_{k=1}^{P_n} \beta_{nk}\boldsymbol{a}\left(\theta_n(t) + \tilde{\theta}_{nk}(t)\right) s_n\left(t - \tau_{nk}\right), \tag{8}$$

$$\boldsymbol{x}(t) = \left[x_1(t), \cdots, x_M(t)\right]^T, \boldsymbol{v}(t) = \left[v_1(t), \cdots, v_M(t)\right]^T$$

$$\boldsymbol{a}(\theta) = \left[1, e^{j\xi\sin\theta}, \cdots, e^{j\xi(M-1)\sin\theta}\right]^T, \ \xi = 2\pi D/\lambda$$

where $\boldsymbol{y}(t)=[y_1(t),\cdots, y_M(t)]^T$ is the $M\times 1$ vector comprising a complex envelope of the observed signal, while β_{nk}, τ_{nk}, and $\theta_n(t)+\tilde{\theta}_{nk}(t)$ are the amplitude, delay time, and direction-of-arrival, respectively, of the k-th arriving signal originally sent from the n-th signal. Pn is the sum of local scattering signals from the n-th signal source; $\boldsymbol{v}(t)$ is the $M\times 1$ observed noise vector composed of white noise with a mean of zero and variance of σ_v^2, having no correlation with $s_n(t)$; and λ is the wavelength of the carrier.

Since the base station is installed in a high location above the level of the mobile terminal in the proposed system, we assume that the angle spread of signals transmitted to the base station is relatively small. In other words, we assume that the base station is located away from the mobile terminal and its surroundings, so the signal scattering occurs primarily in the vicinity of the mobile terminal itself. The model presented in Reference[15] is used to analyze the local scattering signal. The signal delay can be approximated by a phase shift such as $s_n(t-\tau_{nk}) \simeq s_n(t)\, e^{-j2\pi f_c \tau_{nk}}$ and is provided

by Taylor expansion as below:

$$\begin{aligned}\boldsymbol{x}(t) &= \sum_{n=1}^{N}\sum_{k=1}^{P_n}\beta_{nk}e^{-2\pi f_c\tau_{nk}}\left(\boldsymbol{a}(\theta_n(t))+\tilde{\theta}_{nk}\boldsymbol{d}(\theta_n(t))\right)s_n(t),\\ &= \sum_{n=1}^{N}\left\{\varphi_n\boldsymbol{a}(\theta_n(t))+\zeta_n\boldsymbol{d}(\theta_n(t))\right\}s_n(t)\\ \varphi_n &= \sum_{k=1}^{P_n}\beta_{nk}e^{-j2\pi f_c\tau_{nk}}\ ,\quad \zeta_n = \sum_{k=1}^{P_n}\beta_{nk}e^{-j2\pi f_c\tau_{nk}}\tilde{\theta}_{nk}\\ \boldsymbol{d}(\theta) &= \frac{d\boldsymbol{a}(\theta)}{d\theta} = \left[0,\cdots,j\xi(M-1)\cos\theta e^{j\xi(M-1)\sin\theta}\right]^T\end{aligned} \tag{9}$$

where f_c is the frequency of the carrier and ψ_n is a non-zero number including the complex amplitude of the n-th signal. Then the steering vector is re-defined as described by equation (10).

$$\tilde{\boldsymbol{a}}(\theta_n(t)) \triangleq \boldsymbol{a}(\theta_n(t))+\gamma_n\boldsymbol{d}(\theta_n(t)) \tag{10}$$

This equation contains a newly-defined scattering parameter, $\gamma_n = \xi_n/\psi_n$. Assuming that ξ and $|\gamma_n|$ are small values, the m-th element of $\tilde{a}(\theta_n(t))$ in equation (10) can be approximated as follows:

$$\begin{aligned}\left[\tilde{\boldsymbol{a}}(\theta_n(t))\right]_m &= e^{j\xi(m-1)\sin\theta_n(t)}\left(1+j\gamma_n\xi(m-1)\cos\theta_n(t)\right)\\ &\approx e^{j\xi(m-1)\sin\theta_n(t)}e^{j\gamma_n\xi(m-1)\cos\theta_n(t)}\\ &= b_{mn}(t)\end{aligned} \tag{11}$$

An array-antenna signal-receiving model taking the local scattering effect into account can be defined as follows:

$$\boldsymbol{y}(t) = \boldsymbol{x}(t)+\boldsymbol{v}(t) \tag{12}$$

$$\boldsymbol{x}(t) = \sum_{n=1}^{N}\boldsymbol{b}(\theta_n(t))s_n(t) \tag{13}$$

$$\boldsymbol{b}(\theta_n(t)) = \left[1,\cdots,e^{j(M-1)\xi\{\sin\theta_n(t)+\gamma_n\cos\theta_n(t)\}}\right]^T \tag{14}$$

5.3 Estimation of the direction-of-arrival

This section describes the methodology to estimate the direction-of-arrival of signals sent from a moving target utilizing the above local scattering model. Fig.12 is a schematic diagram briefly illustrating the algorithm employed in this method. Using sampling interval T_s and index k, continuous time is converted into discrete time, $t = kT_s$. Assume that the trace of a traveling signal over the short term can be approximated by a straight line, as follows:

$$\begin{aligned}&\theta_n(k-l) \approx \theta_n(k-l|k) = \theta_n(k)-\alpha_n(k)lT_s,\\ &n=1,\cdots,N,\ l=1,\cdots,k-1\end{aligned} \tag{15}$$

where $\alpha_n(k)$ is the angular velocity of the n-th target at time k. Assuming that the value of $j(m-1)\xi\alpha_n(k)lT_s$ is very small, $b_{mn}(k-l|k)$ in equation (11) is approximated as shown by equation (16).

$$\begin{aligned}b_{mn}(k-l|k) &= e^{j(m-1)\xi\left(\sin\theta_n(k-l|k)+\gamma_n\cos\theta_n(k-l|k)\right)}\\ &= e^{j(m-1)\xi\left\{\sin\left(\theta_n(k)-\alpha_n(k)lT_s\right)+\gamma_n\cos\left(\theta_n(k)-\alpha_n(k)lT_s\right)\right\}}\\ &\approx e^{j(m-1)\xi\left\{\sin\theta_n(k)+\gamma_n\cos\theta_n(k)\right\}}\left\{1-j(m-1)\xi\alpha_n(k)lT_s\cos\theta_n(k)\right\}\cdot\\ &\quad\left\{1+j(m-1)\xi\gamma_n\alpha_n(k)lT_s\sin\theta_n(k)\right\}\\ &\approx e^{j(m-1)\xi\left\{\sin\theta_n(k)+\gamma_n\cos\theta_n(k)\right\}}\\ &\quad\left[1-j(m-1)\xi\alpha_n(k)lT_s\left\{\cos\theta_n(k)-\gamma_n\sin\theta_n(k)\right\}\right]\end{aligned} \tag{16}$$

Then, a cost function $J(k)$ is defined as shown below to provide the weighted sum of the residual error functions, as follows.

$$\begin{aligned}J(k) &= \sum_{l=0}^{k-1}\mu_{k-l,k}\left\|\boldsymbol{r}(k-l|k)\right\|^2\\ \boldsymbol{r}(k-l|k) &= \boldsymbol{y}(k-l)-\hat{\boldsymbol{x}}(k-l|k)\\ \hat{\boldsymbol{x}}(k-l|k) &= \sum_{n=1}^{N}\boldsymbol{b}\left(\hat{\theta}_n(k-l|k)\right)\hat{s}_n(k-l)\\ \mu_{k-l,k} &= \rho_k\mu_{k-l,k-1},\ \mu_{k,k}=1\end{aligned} \tag{17}$$

where ρ_k is the forgetting factor at time k and $0 < \rho_k \leq 1$.

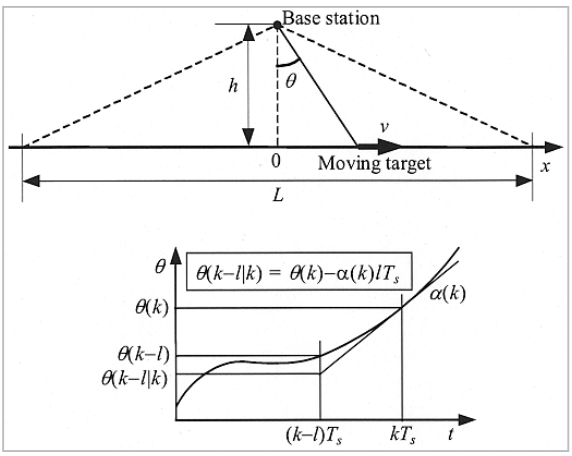

Fig.12 *Linear approximation model for estimation of the direction-of-arrival*

The direction-of-arrival and the angular velocity are provided by minimizing $J(k)$.

Angular velocity $\alpha_n(k)$ is a linear parameter of $J(k)$, while direction-of-arrival $\theta_n(k)$ is a nonlinear parameter. Thus, $\alpha_n(k)$ is obtained by the least-square, and $\theta_n(k)$ is calculated by a Newton-type recursive algorithm.

First, the equation for calculating $\alpha_n(k)$, which minimizes $J(k)$, is derived as follows. Specifically, it is given when $J(k)$ differentiated with respect to $\alpha_n(k)$ equals zero.

$$\frac{\partial J(k)}{\partial \alpha_n(k)} = -2\sum_{l=0}^{k-1}\mu_{k-l,k}\,\mathrm{Re}\left[\boldsymbol{r}^H(k-l\,|\,k)\left\{\hat{s}_n(k-l)\frac{\partial \hat{\boldsymbol{b}}_n(k-l\,|\,k)}{\partial \hat{\alpha}_n(k)}\right\}\right] = 0, \qquad n=1,\cdots,N$$

$$\frac{\partial \hat{b}_{mn}(k-l\,|\,k)}{\partial \hat{\alpha}_n(k)} = e^{j(m-1)\xi\{\sin\hat{\theta}_n(k)+\gamma_n\cos\hat{\theta}_n(k)\}} \cdot\Big[-j(m-1)\xi l t\left\{\cos\hat{\theta}_n(k)-\gamma_n\sin\hat{\theta}_n(k)\right\} +2(m-1)^2\xi^2\gamma_n\hat{\alpha}_n(k)l^2T_s^2\cos\hat{\theta}_n(k)\sin\hat{\theta}_n(k)\Big] \tag{18}$$

Then, the angular velocity is expressed by the following equation.

$$\hat{\alpha}_n(k) = \frac{u_n(k)}{v_n(k)}, \qquad n=1,\cdots,N \tag{19}$$

$$u_n(k) = -\mathrm{Re}\left[\sum_{m=1}^{M} c_m T_s A_n(k)\omega_{mn}^{(1)}(k) \left\{\sum_{\substack{p=1\\ p\neq n}}^{N}\omega_{mp}^{(1)*}(k)\left(c_m T_s\omega_p^{(2)}(k)f_{pn}^{(5)}(k)-jf_{pn}^{(4)}(k)\right)+jf_{mn}^{(2)}\right\} - j\omega_{mn}^{(1)*}f_{nn}^{(4)}\right]$$

$$v_n(k) = M_2\left\{\xi T_s\left|A_n(k)\right|\right\}^2 f_{nn}^{(5)}(k),$$

$$A_n(k) = \cos\hat{\theta}_n(k)-\gamma_n\sin\hat{\theta}_n(k), \quad B_n(k) = \sin\hat{\theta}_n(k)+\gamma_n\cos\hat{\theta}_n(k),$$

$$c_m = (m-1)\xi, \quad \omega_{mn}^{(1)} = e^{j(m-1)\xi B_n(k)}, \quad \omega_n^{(2)} = \hat{\alpha}_n(k)A_n(k),$$

$$\omega_n^{(3)}(k) = \hat{\alpha}_n(k)\left\{B_n(k)-jc_m A_n(k)A_n(k)\right\}, \quad M_2 = \sum_{m=1}^{M}(m-1)\omega_{mn}^{(1)}\omega_{mn}^{(1)*}$$

$$f_{mn}^{(1)}(k) = \sum_{l=0}^{k-1}\mu_{k-l,k}y_m^*(k-l)\hat{s}_n(k-l) = y_m^*(k)\hat{s}_n(k)+\rho_k f_{mn}^{(1)}(k-1),$$

$$f_{mn}^{(2)}(k) = \sum_{l=0}^{k-1}\mu_{k-l,k}ly_m^*(k-l)\hat{s}_n(k-l) = \rho_k\left\{f_{mn}^{(2)}(k-1)+f_{mn}^{(1)}(k-1)\right\},$$

$$f_{pn}^{(3)}(k) = \sum_{l=0}^{k-1}\mu_{k-l,k}\hat{s}_p^*(k-l)\hat{s}_n(k-l) = \hat{s}_p^*(k)\hat{s}_n(k)+\rho_k f_{pn}^{(3)}(k-1),$$

$$f_{pn}^{(4)}(k) = \sum_{l=0}^{k-1}\mu_{k-l,k}l\hat{s}_p^*(k-l)\hat{s}_n(k-l) = \rho_k\left\{f_{pn}^{(4)}(k-1)+f_{pn}^{(3)}(k-1)\right\},$$

$$f_{pn}^{(5)}(k) = \sum_{l=0}^{k-1}\mu_{k-l,k}l^2\hat{s}_p^*(k-l)\hat{s}_n(k-l) = \rho_k\left\{f_{pn}^{(5)}(k-1)+2f_{pn}^{(4)}(k-1)+f_{pn}^{(3)}(k-1)\right\},$$

Now consider direction-of-arrival $\theta_n(k)$, which minimizes cost function $J(k)$. Since direction-of-arrival $\theta_n(k)$ is a nonlinear parameter, it is derived from the following Newton-type recursive algorithm.

$$\hat{\boldsymbol{\theta}}(k) = \hat{\boldsymbol{\theta}}(k-1)-\eta\boldsymbol{H}^{-1}(k)\boldsymbol{g}(k) \tag{20}$$

where $\boldsymbol{\theta}_n(k) = [\theta_1(t), \cdots, \theta_N(t)]^T$ is the $N\times 1$ arrival-direction vector, η the step size, and $0 < \eta \leq 1$. $\boldsymbol{g}(k)$ and $\boldsymbol{H}(k)$ are the gradient vector and Hessian matrix of $J(k)$, respectively, which are expressed as below:

$$\boldsymbol{g}(k) = \frac{\partial J(k)}{\partial \hat{\boldsymbol{\theta}}(k)} = \left[g_1(k), g_2(k), \cdots, g_N(k)\right]^T \tag{21}$$

$$\boldsymbol{H}(k) = \frac{\partial^2 J(k)}{\partial \hat{\boldsymbol{\theta}}(k)\partial \hat{\boldsymbol{\theta}}^T(k)} = \begin{bmatrix} \vdots & \\ \cdots & h_{pn}(k) \quad \cdots \\ \vdots & \end{bmatrix} \tag{22}$$

$$g_n(k) = -2\,\mathrm{Re}\left[\sum_{m=1}^{M} jc_m\omega_{mn}^{(1)}(k)\left\{g_n(k)-\sum_{p=1}^{N}\omega_{mp}^{(1)*}(k)g_{pn}^{(2)}(k)\right\}\right],$$

$$h_{pn}(k) = 2\,\mathrm{Re}\left[\sum_{m=1}^{M} c_m^2\omega_{mn}^{(1)}(k)\omega_{mp}^{(1)*}(k)h_{pn}^{(1)}\right],$$

$$g_n^{(1)}(k) = A_n(k)f_{mn}^{(1)}+T_s\omega_n^{(3)}(k)f_{mn}^{(2)}(k),$$

$$g_{pn}^{(2)}(k) = A_n(k)f_{pn}^{(3)} +T_s\left[\omega_n^{(3)}(k)+jc_m A_n(k)\omega_p^{(2)}(k)\right] f_{pn}^{(4)}(k) +jc_m T_s^2\omega_p^{(2)*}(k)\omega_n^{(3)}(k)f_{pn}^{(5)}(k),$$

$$h_{pn}^{(1)}(k) = A_p^*(k)A_n(k)f_{pn}^{(3)}(k) +T_s\left[A_n(k)\omega_p^{(3)*}(k)+A_p^*(k)\omega_n^{(3)}(k)\right] f_{pn}^{(4)}(k) +T_s^2\omega_p^{(3)*}(k)\omega_n^{(3)}(k)f_{pn}^{(5)}(k).$$

Summarizing the above results, the following recursive procedures are derived:

1. Make $\hat{\boldsymbol{\theta}}(k-1)$ the estimated direction-of-arrival and $\hat{\boldsymbol{\alpha}}(k-1) = \hat{\alpha}_1[(k-1), \hat{\alpha}_2(k-1),$ L, $\hat{\alpha}(k-1)]^T$ the angular velocity estimate vector at time k–1.
2. Calculate the provisional direction-of-arrival $\hat{\boldsymbol{\theta}}(k)$ from $\hat{\boldsymbol{\theta}}(k-1)$ and $\hat{\boldsymbol{\alpha}}(k-1)$.
3. Predict $\hat{\boldsymbol{s}}(k)$, which has a complex amplitude, based on the direction-of-arrival $\hat{\boldsymbol{\theta}}(k)$ estimated in Step 2, and on the least square.
4. Renew $\hat{\boldsymbol{\alpha}}(k)$ and $\hat{\boldsymbol{\theta}}(k)$ using equations (19) and (20), respectively.
5. Increment k to $k+1$, and return to Step 2.

The convexity of the cost function with

respect to the directions-of-arrival in the neighborhood of their true values can be proved by the same method shown in Reference[7]. Therefore, a value close to the true value must be provided as the initial value to allow a precise estimate to be made by the above method. Another method (such as MUSIC[17]) may be used to obtain the initial estimated value.

5.4 Estimation of the scattering parameter

In general, scattering parameter γ is an unknown factor estimated from the observed signal. As scattering parameter $\gamma_n(k)$ in equation (14) is a non-linear parameter of J(k), a recursive algorithm or other method is used to estimate the scattering parameter. Several methods have been proposed for estimating the scattering parameter, as presented in References[15] and[21]. However, the method introduced in Reference[15] is not suitable for real-time tracking algorithms, as it requires a large amount of calculations, including that for eigenvalue decomposition. The other method explained in Reference[21] requires a certain amount of observed data and recursive processing to obtain the scattering parameter. Thus, in this paper, we have slightly modified the model used in equation (10) to linearize the scattering parameter in *J(k)*.

Since the steering vector can be given by the following equation:

$$\tilde{\boldsymbol{a}}\left(\theta_n(t)\right) \triangleq \boldsymbol{a}\left(\theta_n(t)\right) + \gamma_n \boldsymbol{d}\left(\theta_n(t)\right)$$

we assume that parameter γ_n and $\alpha_n l T_s$ provide very small values in the effective time window given by the forgetting factor. Then, the steering vector in equation (10) is approximated as below:

$$\begin{aligned}
\tilde{\boldsymbol{a}}\left(\theta_n(k-l)\right) &\triangleq \boldsymbol{a}\left(\theta_n(k-l)\right) + \gamma_n \boldsymbol{d}\left(\theta_n(k-l)\right) \\
&\approx \boldsymbol{a}\left(\theta_n(k) - \alpha_n(k) l T_s\right) + \gamma_n \boldsymbol{d}\left(\theta_n(k) - \alpha_n(k) l T_s\right) \\
&\approx \boldsymbol{a}\left(\theta_n(k)\right) - \alpha_n(k) l T_s \boldsymbol{d}\left(\theta_n(k)\right) \\
&\quad + \gamma_n \left[\boldsymbol{d}\left(\theta_n(k)\right) - \alpha_n(k) l T_s \frac{\partial}{\partial \theta_n(k)} \boldsymbol{d}\left(\theta_n(k)\right) \right] \\
&\approx \boldsymbol{a}\left(\theta_n(k)\right) - \alpha_n(k) l T_s \boldsymbol{d}\left(\theta_n(k)\right) + \gamma_n \boldsymbol{d}\left(\theta_n(k)\right) \\
&\triangleq \tilde{\boldsymbol{b}}\left(\theta_n(k-l)\right)
\end{aligned} \tag{23}$$

This derivation is made by discarding higher-order terms with respect to α_n and γ_n so that they can be linearized. As a result of the modification given by equation (23), parameter $\gamma_n(k)$ can be estimated by the same method as that for the estimation of $\alpha_n(k)$.

Next, we define a new evaluation function similar to equation (17).

$$J_2(k) = \sum_{l=0}^{k-1} \tilde{\mu}_{k-l,k} \left\| \tilde{\boldsymbol{r}}\left(k-l|k\right) \right\|^2 \tag{24}$$

$$\tilde{\boldsymbol{r}}\left(k-l|k\right) = \boldsymbol{y}\left(k-l\right) - \hat{\tilde{\boldsymbol{x}}}\left(k-l|k\right) \tag{25}$$

$$\hat{\tilde{\boldsymbol{x}}}\left(k-l|k\right) = \sum_{n=1}^{N} \tilde{\boldsymbol{b}}\left(\hat{\theta}_n\left(k-l|k\right)\right) \hat{\boldsymbol{s}}_n\left(k-l\right) \tag{26}$$

$$\tilde{\mu}_{k-l,k} = \tilde{\rho}_k \tilde{\mu}_{k-l,k-1}, \quad \tilde{\mu}_{k,k} = 1$$

Then, $\gamma_n(k)$, which minimizes $J_2(k)$, is given by solving the following equation, as $\gamma_n(k)$ is a complex number and $\alpha_n(k)$ is a real number.

$$\begin{aligned}
&\frac{\partial J_2(k)}{\partial \gamma_n(k)} \\
&= -2 \sum_{l=0}^{k-1} \tilde{\mu}_{k-l,k} \operatorname{Re}\left[\tilde{\boldsymbol{r}}^H\left(k-l|k\right) \left\{ \hat{s}_n\left(k-l\right) \frac{\partial \hat{\tilde{\boldsymbol{b}}}_n\left(k-l|k\right)}{\partial \hat{\gamma}_n(k)} \right\}^* \right] \\
&= 0, \quad n = 1, \cdots, N.
\end{aligned} \tag{27}$$

Consequently, the scattering parameter can be estimated as follows:

$$\operatorname{Re}\left\{\hat{\gamma}_n(k)\right\} = \frac{\tilde{u}_n^R(k)}{\tilde{v}_n(k)}, \quad n = 1, \cdots, N$$

$$\operatorname{Im}\left\{\hat{\gamma}_n(k)\right\} = \frac{\tilde{u}_n^I(k)}{\tilde{v}_n(k)}, \quad n = 1, \cdots, N$$

$$\begin{aligned}
\tilde{u}_n^R(k) = \operatorname{Re}\Bigg[&\sum_{l=0}^{k-1} \mu_{k-l,k} \left\{ \tilde{\boldsymbol{r}}\left(k-l|k\right) + \hat{s}_n\left(k-l\right) \hat{\tilde{\boldsymbol{b}}}_n\left(k-l|k\right) \right\}^H \\
&\left\{ \hat{s}_n\left(k-l\right) \boldsymbol{d}\left(\theta_n(k)\right) \right\}^* \Bigg]
\end{aligned}$$

$$\begin{aligned}
\tilde{u}_n^I(k) = \operatorname{Re}\Bigg[&\sum_{l=0}^{k-1} \mu_{k-l,k} \left\{ \tilde{\boldsymbol{r}}\left(k-l|k\right) + \hat{s}_n\left(k-l\right) \hat{\tilde{\boldsymbol{b}}}_n\left(k-l|k\right) \right\}^H \\
&\left\{ j \hat{s}_n\left(k-l\right) \boldsymbol{d}\left(\theta_n(k)\right) \right\}^* \Bigg]
\end{aligned}$$

$$\tilde{v}_n(k) = \tilde{M}_2 \left\{ \xi \cos \hat{\theta}_n(k) \right\}^2 \sum_{l=0}^{k-1} \tilde{\mu}_{k-l,k} \left| \hat{s}_n\left(k-l\right) \right|^2,$$

$$\tilde{M}_2 = \frac{M(M-1)(2M-1)}{6}$$

5.5 Results of the simulation study

We use a linear array antenna in which four elements are arranged at equal intervals of half the wavelength of the carrier in our simulation study. We assume that the observed signals contain 50 local scattering waves and that the incident angles show a normal distribution with standard deviation δ. The standard deviations of the incident angles were set at 2, 5, and 8 degrees based on Reference[22]. Other simulation conditions are listed on Table 2.

Table 2 *Simulation parameters*

Modulation scheme	QPSK
Wavelength λ	5mm
Pattern of the element antenna	Isotropic
Sampling rates	5kHz
Initial velocity of the mobile	25m/s
Step size η	0.30
Forgetting factor ρ	0.98
Base station height h	5m
Service distance L	50m
Standard deviation δ	2°, 5°, 8°

This simulation takes into account only free-space propagation loss and the Doppler effect, so CNR of the output of each antenna element may change as the target (mobile terminal) moves.

In the simulation below, CNR is set at 5dB for each element when the terminal is located at x = –25 m.

Fig.13 shows the true direction-of-arrival (dotted line) and its estimate (solid line) obtained by the proposed method, in a case in which a single mobile terminal is used. The standard deviation of the direction-of-arrivals was $\delta = 5$ degrees, and the initial speed was $a_{cc} = 0$ m/s^2 and –10m/s^2. Fig.14 demonstrates the square errors in the estimation of the direction-of-arrival by our method (solid line) and that based on Reference[8] (dot-dash line). For the simulation, we assumed that the initial direction-of-arrival and initial angular velocity were known in advance. Table 3 lists the mean square errors (MSE) in the simulation.

Fig.13 indicates that the proposed algorithm can precisely and stably track the mobile

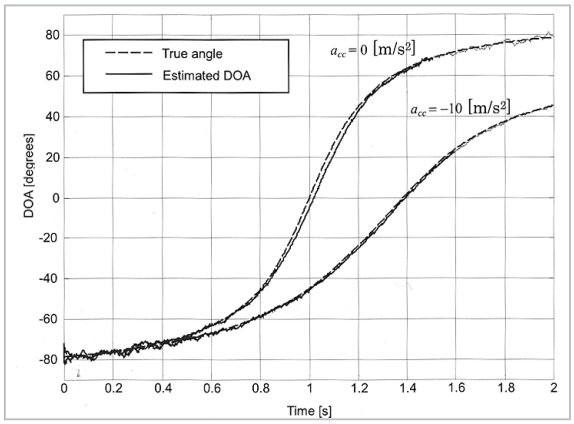

Fig.13 *Estimation of the direction-of-arrival of signals sent from a single mobile terminal*

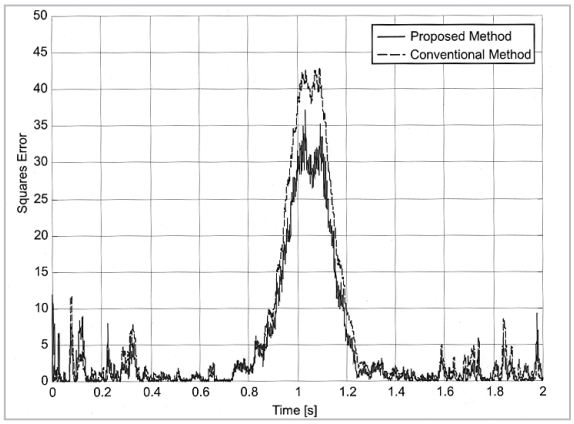

Fig.14 *Mean-square errors of the estimates*

Table 3 *Mean-square error of estimates of the direction-of-arrival Proposed method, Method in Reference* [8]

Aacc=0m/s2	δ=2°	δ=5°	δ=8°
Proposed method	1.97	4.38	4.91
Method in Reference [8]	2.81	5.70	8.76

terminal despite a limited number of antenna elements. Fig.14 also indicates that the proposed method can estimate the direction-of-arrival with higher accuracy than the method presented in Reference[8]. In addition, the results in Table 3 show that the proposed method is less affected by the local-scattering effect.

6 Field experiment

6.1 Tracking signal-processing device

We executed the proposed algorithm utilizing a digital-signal-processor (DSP) for the implementation of a real-time estimate of the

direction-of-arrival. As shown in Fig.15, the DSP is composed of A/D converters, a main processor for executing the algorithm, and a sub-processor (TMS320C40) used for system control or as an inter-computer interface. The main processor was a Compaq (formerly DEC) Alpha 500-MHz processor. Main processors can be added depending on the amount of calculation required.

Prior to the actual field experiment, we constructed an array-data simulator to carry out preliminary experiments in order to check the performance of the developed tracking system. This array-data simulator can provide simulated signal data received in the array antenna and change the direction-of-arrival and intensity of signals sent from a virtual mobile terminal over time. Fig.16 shows the results of a tracking test on a virtual mobile terminal with a speed set at 180 km/h. Its antenna height, signal sampling rate, and CNR were set at 5 m, 5 kHz, and 3 dB, respectively. Local-scattering effects were not considered in that experiment. The experimental results indicate that the tracking system can precisely estimate the direction-of-arrival on a real-time basis.

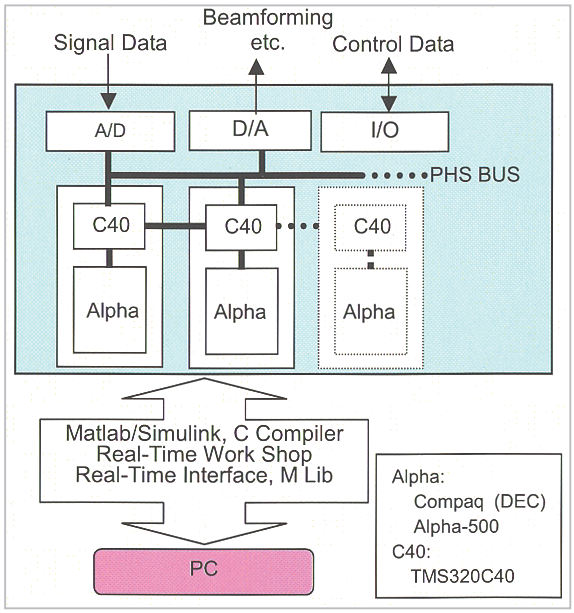

Fig.15 *DSP for estimation of the direction-of-arrival and beamforming*

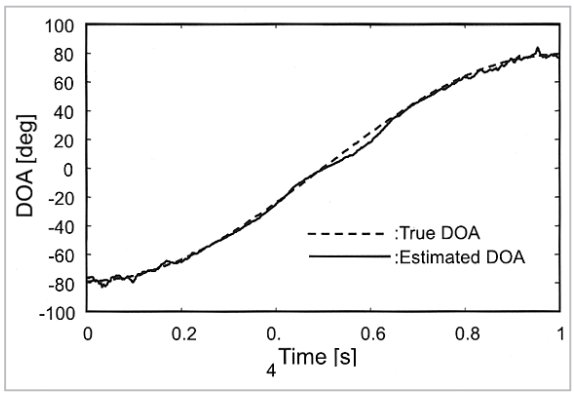

Fig.16 *Estimation of the direction-of-arrival using DSP*

6.2 Experimental system

We conducted field experiments in a test course in order to check the effectiveness of the tracking algorithm and the practical capabilities of the proposed millimeter-wave broadband wireless access system[20]. Fig.17 illustrates the configuration of the experimental system. The mobile terminal is equipped with a signal generator and a micro-strip antenna.

The base station is composed of an array antenna, frequency converters, E/O converters, and multiplexers. The base station is equipped with the microstrip-type array antenna described in Section 4. The control station is composed of demultiplexers, O/E converters, orthogonal detectors, A/D converters, DSP, and PC. The tracking algorithm proposed in Section 5 is installed in DSP. The estimation results for direction-of-arrival are saved to the PC. In the experiments, we used an estimation model that ignored local-scattering effects. This is due to the fact that a model that takes local-scattering effects into account must estimate the scattering parameter in addition to the direction-of-arrival and angular velocity, and the required amount of calculations is beyond the capability of the current system. Fig.18 shows the geographical relationships between the base station and the mobile terminal, while Fig.19 shows the field experiment. In this experiment, we mounted the antenna of the base station at roadside, in consideration of the structure of the measurement system. As investigated in Section 3 with regard to the antenna configuration for

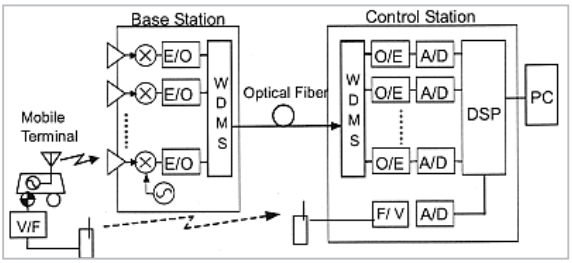

Fig.17 *Configuration of the experimental system*

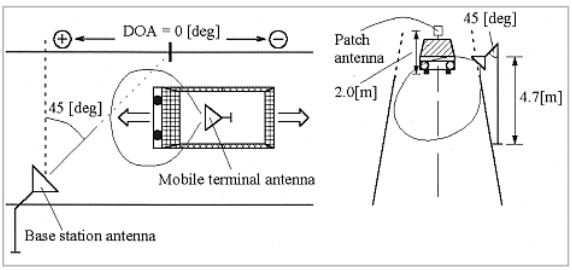

Fig.18 *Geographic relationships between the base station and mobile terminal*

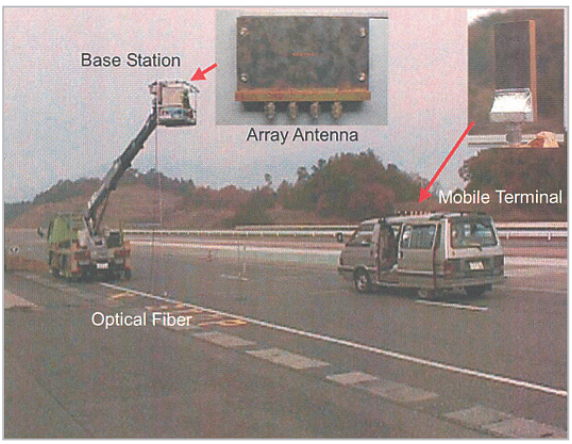

Fig.19 *Field experiment*

the base station and mobile terminal, the installation angles of the base-station antenna were set such that ϕ_B = 45 degrees toward the mobile terminal and θ_B = 45 degrees in the vertical direction. In order to ensure a CNR margin slightly greater than the theoretical value required for estimation of the direction-of-arrival of signals sent from the mobile terminal, we set the angle of the mobile-terminal antenna at ϕ_M = 90 degrees. The antennas of the mobile terminal and the base station were 2 m and 4.7 m in height, respectively. The carrier frequency was 59.5 GHz, the intermediate frequency was 1.5 GHz, and the sampling rate for receiving signals was set to 1 kHz. Non-modulation signals were used for transmission.

6.3 Results of the field experiment

Figs.20 and 21 show the direction estimates of signals sent from the mobile terminal obtained in the experiment. The thin line indicates the actual angles, while the thick line indicates the estimates. The horizontal axis indicates the elapsed time in seconds, and the vertical axis indicates the direction-of-arrival of signals received using the base-station antenna. As shown in Fig.20, the mobile terminal was moved around the base station at speeds of approximately 10 km/h. Since the mobile terminal is located far from the base station, the estimates of the direction-of-arrival fluctuate. This is probably due to the

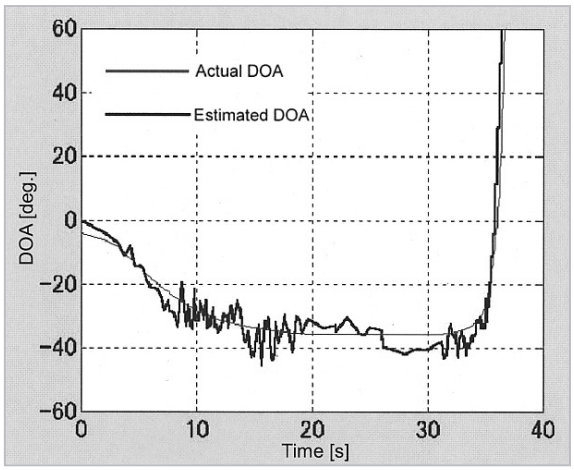

Fig.20 *Estimated direction-of-arrival 1 in the field experiment*

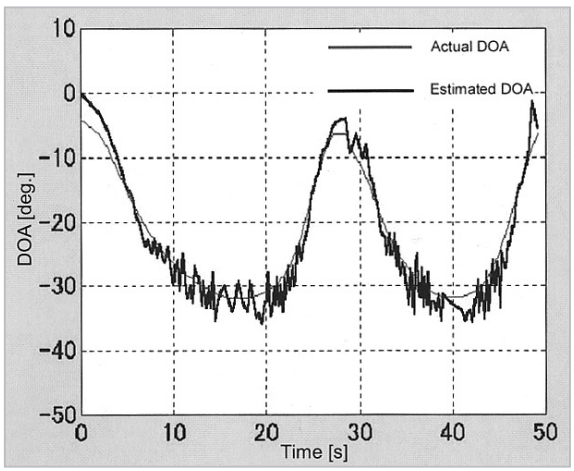

Fig.21 *Estimated direction-of-arrival 2 in the field experiment*

fact that CNR falls as a result of signal decay as the length of the signal path increases. The figures indicate that the direction-of-arrival can be estimated within 5 degrees or less.

In the test shown in Fig.21, the mobile terminal moved to a location 80 m from the point directly under the base station, then approached the base station. Its approach speed during this test reached approximately 55 km/h in the vicinity of the base station. Even when the mobile terminal moves this fast, the proposed system can precisely track the course of the mobile terminal in real-time.

7 Conclusions

In this paper, we proposed a millimeter-wave broadband wireless access system and described a mobile-terminal tracking system and a wavelength-division-multiplexing transmission system equipped with a millimeter-wave array antenna, which we developed. Also proposed was a new mobile-terminal tracking algorithm utilizing a local-scattering model that accounts for the multipath transmission effect. The performance of the proposed system has been confirmed in an experiment for estimating the direction-of-arrival of signals sent from the mobile terminal the millimeter-wave array antenna and the wavelength-division-multiplexing access system. In the future, we plan to focus on research into both the tracking system and data transmission.

Acknowledgment

The authors would like to extend their thanks to Mr. M. Hirakawa, Mr. Y. Okada, Mr. N. Ohmi, and Mr. N. Tago for their collaboration on the experiments.

References

1 "Introduction to Mobile and Wireless ATM," IEEE Communications Magazine, Vol. 35, No. 11, Nov. 1997.

2 "Wireless ATM," IEEE Personal Communications, Vol. 3, No. 4, Aug. 1996.

3 M. Umehira, M. Nakura, H. Sato, and A. Hashimoto, "ATM Wireless Access for Mobile Multimedia: Concept and Architecture," IEEE Personal Communications, Vol. 3, No. 5, Oct. 1996.

4 H. Matsue, M. Umehira, and A. Hashimoto, "Future trend of broadband wireless access systems and their core technologies," MWE`96, WS10-1, 1996.

5 A. Plattner, "Technology and Demonstrator of the RACE Project 'Mobile Broadband System'," 1994 IEEE MTT-S Digest, paper WEID-4, pp. 639-642, 1994.

6 S. Yoshimoto, T. Iwama, H. Tsuji, and J. Xin, "Millimeter-wave broadband wireless access system," MWE'96, WS7-3, 1996.

7 H. Kagiwada, H. Ohmori, and A. Sano, "A recursive algorithm for tracking DOA's of moving targets by using linear approximations," IEICE Trans. Fundamentals,Vol. E-81A, 1998.

8 Y. Okada, H. Tsuji, H. Kagiwada, and A. Sano, "Millimeter-wave broadband wireless access system with tracking technology of moving targets," Proc. 1998 IEEE VTC Conf., pp. 2057-2061, Ottawa, 1998.

9 Y. Okada, H. Tsuji, S. Yoshimoto, H. Kagiwada, and A. Sano, "Tracking Method of Moving Targets for Millimeter-Wave Multimedia Mobile Access Communications System," Technical Report of IEICE, Vol.RCS97, No.194, pp. 83-88, 1997.

10 H. Tsuji, Y. Hase, Y. Okada, M. Hirakawa, and N. Ohmi, "Development of fast mobile tracking system for broadband wireless access," Technical Report of IEICE, Vol.RCS98, No.56, pp.37-42, 1998.

11 H. Tsuji, M. Jansson, A. Sano, and M. Kaveh, "A new approach for tracking mobiles with local scattering modeling," Proc. of IEE EUSIPCO2000 Conf., Tampere, Finland 2000.

12 S. Komaki and E. Ogawa, "Trends of Fiber-Optic Microcellular Radio Communication Networks," IEICE Trans. Electron., Vol.E-79C, No.1, pp.98-104, Jan. 1996.

13 T. Shimura, M. Hirakawa, Y. Okada, N. Ohmi, A. Kamemura, H. Tsuji, and S. Yoshimoto, "Optical wavelength division multiplexed subcarrier transmission for array antenna control," Technical report of IEICE, Vol.MW97-45, pp.63-68, 1997.

14 N. Ohmi, M, Hirakawa, Y. Okada, H. Tsuji, and S. Yoshimoto, "Measurement of the Array Antenna for Millimeter-Wave Multimedia Mobile Access Communication System," IEICE Soc. Conf., B-5-131, Japan, 1997.

15 D. Asztely, B. Ottersten, and A. Swindlehurst, "A generalized array manifold model for local scattering in wireless communications," Proceedings of IEEE international conference on acoustics, speech and signal processing, Munich, Germany, Apr. 1997, Vol.V, pp.4021-4024.

16 L. C. Godara, "Application of antenna arrays to mobile communications, part II: beam-forming and direction-of-arrival considerations," Proc. of IEEE, Vol.85, No.8, pp.1195-1245, Aug. 1997.

17 R. O. Schmidt, "Multiple emitter location and signal parameter estimation." IEEE Trans. Antennas Propagat., Vol. 34, pp. 276-280, 1986.

18 Y. T. Lo and S. W. Lee, "Antenna Handbook," Vol.1, Kluwer Academic Publishers, Jan. 15, 1993.

19 R. C. Johnson and H. Tasik (editor), "Antenna Engineering Handbook," McGrow-Hill. 2nd. Edition, Jan. 1993.

20 H. Mitsuru, Y. Okada, N. Ohmi, N. Tago, H. Tsuji, and H. Ogawa, "Field experiments of direction-of-arrival estimation for millimeter-wave mobile access communication system," Proc. the 2000 IEICE general conf., B-5-106, Mar. 2000.

21 K. Yamada and H. Tsuji, "Array antenna beamforming method using local scattering model," Technical report of IEICE, No. RCS2000-213, Mar. 2001.

22 T. Inoue and Y. Karasawa, "Two-dimensional RAKE reception scheme for DS/CDMA systems in DBF antenna configuration," Proc. 47th VTC, pp. 2228-2232, May 1997.

23 J. G. Proakis, "Digital Communications," McGrow-Hill, 2nd. Edition, 1989.

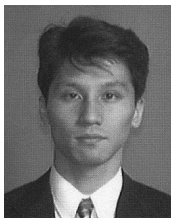

***Hiroyuki TSUJI**, Ph. D.*

Senior Researcher Broadband Wireless Access Systems Group, Yokosuka Radio Communications Research Center

Signal processing in wireless communications

***Hiroyo OGAWA**, Dr. Eng.*

Leader, Broadband Wireless Access Systems Group, Yokosuka Radio Communications Research Center

Multimedia Wireless Access Technology